Electronic Supplementary Material (ESI) for Chemical Communications.

Augmenting metallobasicity to modulate gold hydrogen bonding

Logan T. Maltz, Lewis C. Wilkins and François P. Gabbaï*

Department of Chemistry, Texas A&M University, College Station, Texas 77843-3255, United States

SUPPORTING INFORMATION

This PDF file includes

Contents

Synthetic Details

General Considerations. ((2-diphenylphosphino)phenyl)diphenylmethanol (**1**)[1] and (tht)AuCl (tht = tetrahydrothiophene)[2] were prepared according to literature procedures. All commercially available compounds were used as received. All solvents were ACS reagent grade and used as received. The synthesis of all compounds was carried out on the benchtop under ambient conditions unless otherwise stated. ^{1}H, ^{13}C, and ^{31}P NMR spectra were recorded at 298.0 K on a Bruker Avance Neo 400 spectrometer (400.09 MHz for ^{1}H; 162.00 MHz for $^{31}P\{^{1}H\}$) or at 305.0 K on a Bruker Avance 500 NMR spectrometer (500.13 MHz for ^{1}H; 125.77 MHz for $^{13}C\{^{1}H\}$) equipped with an automated tuning 5 mm $^{1}H/^{13}C/^{15}N$ cold probe. Chemical shifts are given in ppm and are referenced to residual $CHCl_3$ $^{1}H/^{13}C$ solvent signal (7.26/77.16 ppm) or external 85% H_3PO_4 (^{31}P). IR spectra were recorded on a Shimadzu IRAffinity-1S FTIR spectrometer equipped with a Pike MIRacle attenuated total reflectance (ATR) device.

Crystallographic measurements. The crystallographic measurements were performed at 110 K using a Bruker D8 QUEST diffractometer (Mo-Kα radiation, λ = 0.71073 Å) equipped with a Photon III detector. In each case, a specimen of suitable size and quality was selected and mounted onto a nylon loop. Integrated intensity information for each reflection was obtained by reduction of the data frames with either APEX3[3] or CrysAlis RED.[4] The semiempirical method SADABS was applied for the absorption correction.[5] The structures were solved by intrinsic phasing (ShelXT)[6] and refined by the full-matrix least-squares technique against F^2 with anisotropic temperature parameters for all non-hydrogen atoms (ShelXL)[7] using the Olex2-1.5 interface.[8] The hydrogen atoms (except those of the carbinol functionalities in the polymorphs of **3**) were placed in calculated positions and refined using a riding model approximation. Diamond4 was employed for the final data presentation and structure plots. The data has been deposited with the Cambridge Structural Database. CCDC 2178883-2178885 and CCDC 2191898 contain the supplementary crystallographic data for this paper.

Synthesis of 2

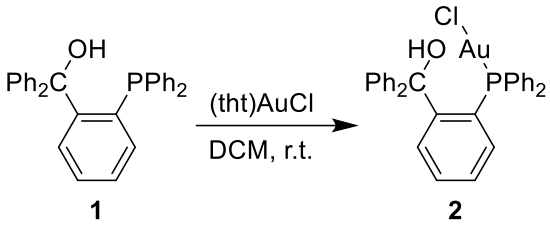

1 **2**

1 (0.2004 g, 0.4508 mmol) was weighed into a tared 20 mL scintillation vial with a stir bar before being dissolved in 2 mL DCM. A solution of tetrahydrothiophene gold(I) chloride (0.1587 g, 0.4950 mmol) in 3 mL DCM was added to the vial containing **1**, quickly producing a clear, colorless solution. The reaction proceeded for about 30 minutes at room temperature before the stir bar was removed and the reaction solution was layered with Et_2O. The supernatant was decanted, and the recrystallized product was triturated with 3 × 3 mL Et_2O. The product was dried *in vacuo*, yielding the final product as a colorless, crystalline solid (0.2157 g, 0.3186 mmol, 71% yield). **^{1}H NMR** (500.13 MHz, $CDCl_3$, 305.0 K) δ (ppm) 7.50-7.45 (m, 4H), 7.41-7.30 (m, 11H), 7.22 (tt, 1H), 7.02-6.97 (m, 5H), 6.96-6.93 (m, 1H), 3.01 (s, 1H, O*H*). **^{13}C{^{1}H} NMR** (125.77 MHz, $CDCl_3$, 305.0 K) δ (ppm) 150.29 (d, J = 8.1 Hz), 148.60 (s), 136.24 (d, J = 7.6), 134.15 (d, J = 14.0 Hz), 132.95 (d, J = 62.6 Hz), 132.78 (s), 131.08 (d, J = 2.3 Hz), 130.50 (d, J = 2.2 Hz), 128.94 (d, J = 11.8 Hz), 128.61 (s), 128.37 (s), 128.24 (s), 127.69 (d, J = 10.0 Hz), 127.55 (d, J = 55.8 Hz), 84.69 (d, J = 0.9 Hz). **^{31}P{^{1}H} NMR** (162.00 MHz, $CDCl_3$, 298.0 K) δ (ppm) 35.74. **Elemental Analysis:** Calculated for $C_{31}H_{25}AuClOP$: C 55.00, H 3.72. Found: C 54.99, H 3.70.

Synthesis of 3

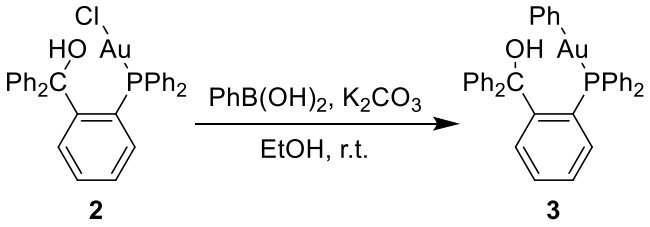

2 **3**

$PhB(OH)_2$ (0.0199 g, 0.163 mmol) was dissolved in EtOH (0.8 mL, 200 proof), producing a clear, colorless solution. This solution was added to a 1 dram vial containing **2** (0.0998 g, 0.147 mmol) and K_2CO_3 (0.0612 g, 0.443 mmol), immediately producing an opaque gray suspension. This reaction mixture was allowed to stir overnight, producing a white suspension. The mixture was dissolved in 1 mL DCM which was filtered through a pad of basic alumina and thoroughly eluted with DCM (3 × 1.5 mL). The solvent was removed *in vacuo*, yielding a bright white powder. This powder was triturated with pentane (3 × 3 mL) and again dried *in vacuo*, ultimately yielding **3** as a bright white powder (0.0916 g, 0.127 mmol, 86% yield). Single crystals of **3** were obtained as colorless blocks via layering of pentane over a DCM solution of the compound in a freezer. A second polymorph containing interstitial solvent was obtained via this method. A third polymorph was obtained by recrystallizing at room temperature instead. **^{1}H NMR** (500.13 MHz, $CDCl_3$, 305.0 K): δ 7.60-7.55 (m, 4H), 7.47-7.43 (m, 2H), 7.41-7.38 (m, 4H), 7.30 (t, 1H), 7.26-7.24 (m, 6H), 7.20 (t, 1H), 7.15-7.04 (m, 8H), 7.03-6.97 (m, 3H), 3.86 (d, *J* = 2.3 Hz, 1H, O*H*). **^{13}C{^{1}H} NMR** (125.77 MHz, $CDCl_3$, 305.0 K): δ 169.49 (d, *J* = 122.1 Hz), 150.27 (d, *J* = 9.1 Hz), 147.59 (s), 139.70 (s), 136.45 (d, *J* = 5.5 Hz), 134.51 (d, J = 13.8 Hz), 134.46 (d, J = 49.4 Hz), 132.73 (d, *J* = 7.8 Hz), 130.48 (d, *J* = 2.2 Hz), 129.80 (d, *J* = 1.7 Hz), 129.35 (d, *J* = 40.8 Hz), 128.82 (d, *J* = 10.5 Hz), 128.41 (s), 128.28 (s), 127.87 (s), 127.51 (d, *J* = 7.5 Hz), 127.15 (d, *J* = 6.8 Hz), 125.50 (s), 84.94 (s). **^{31}P{^{1}H} NMR** (162.00 MHz, $CDCl_3$, 298.0 K): δ 48.43. **Elemental Analysis:** Calculated for $C_{37}H_{30}AuOP$: C 61.84, H 4.21. Found: C 61.77, H 4.19.

Experimental Spectra

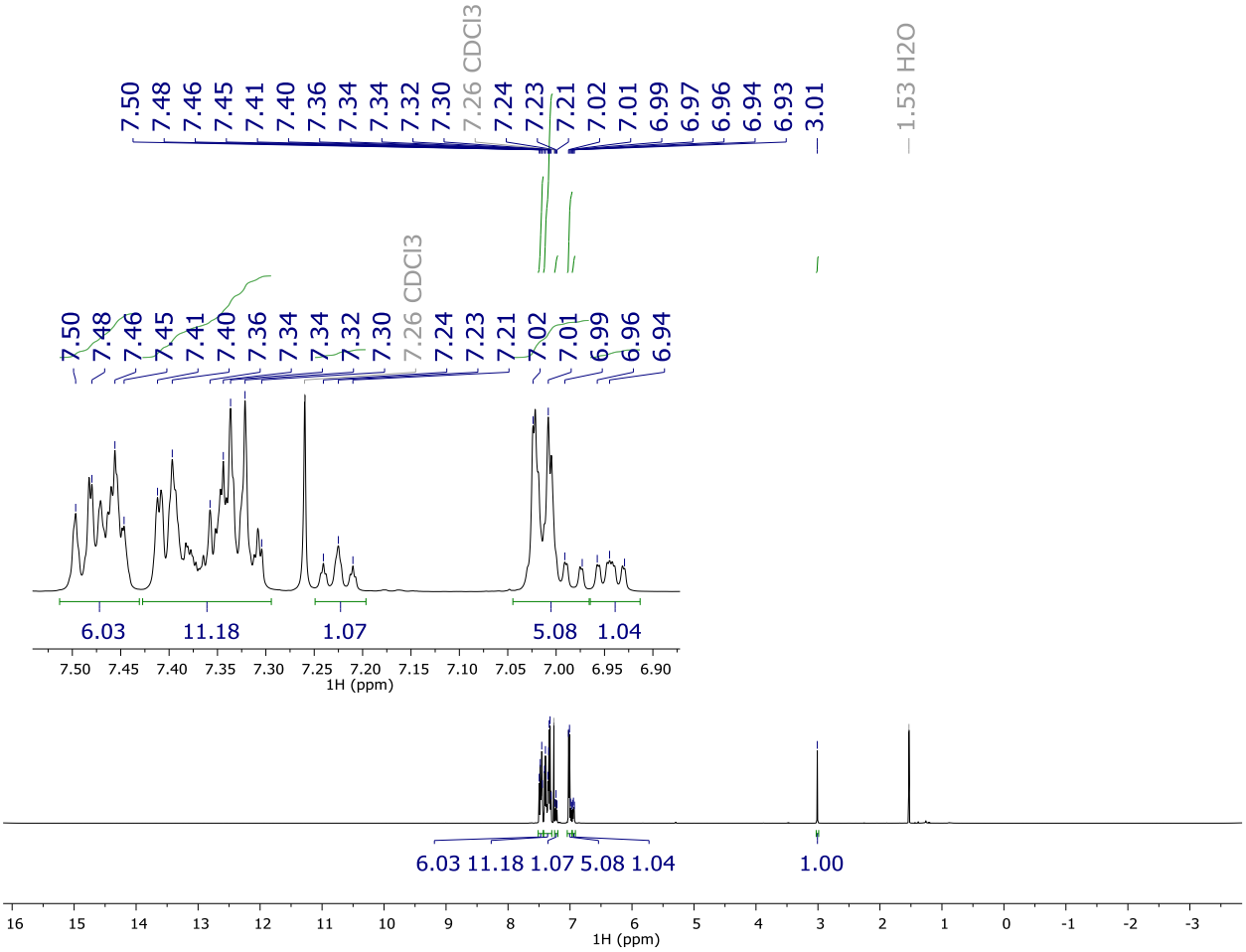

Figure S1. ^{1}H NMR spectrum of **2** in $CDCl_3$.

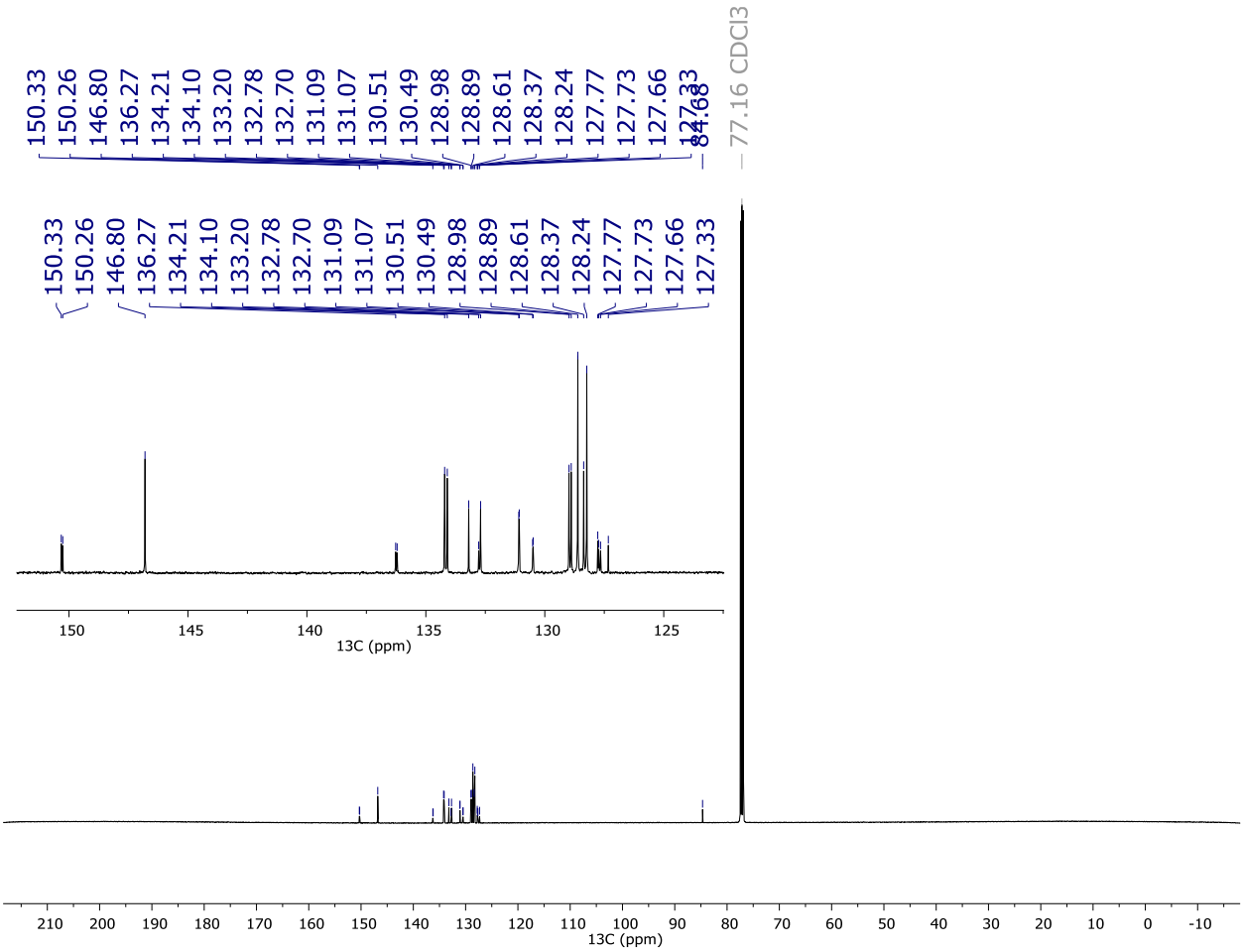

Figure S2. $^{13}C\{^{1}H\}$ NMR spectrum of **2** in $CDCl_3$.

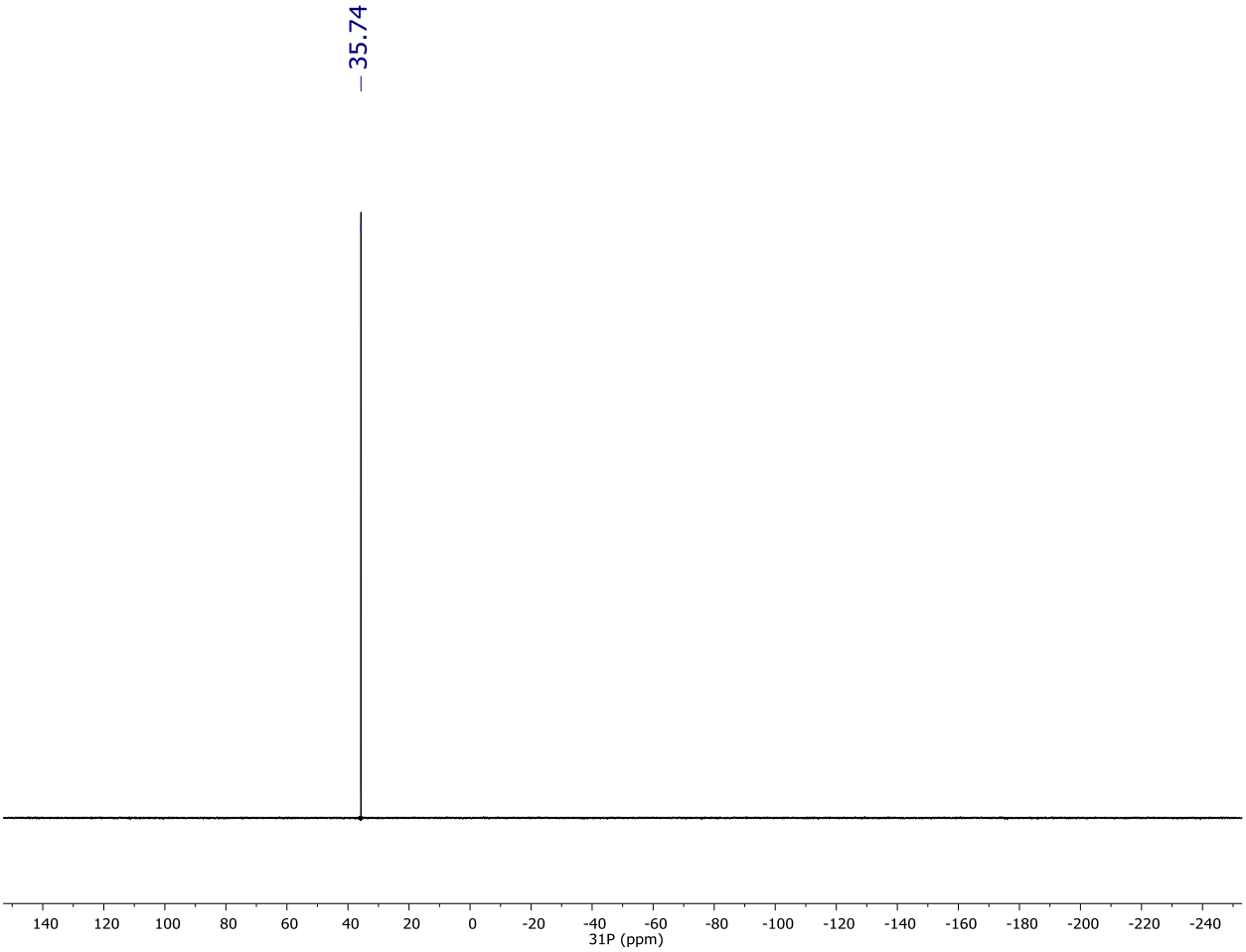

Figure S3. $^{31}P\{^{1}H\}$ NMR spectrum of **2** in $CDCl_3$.

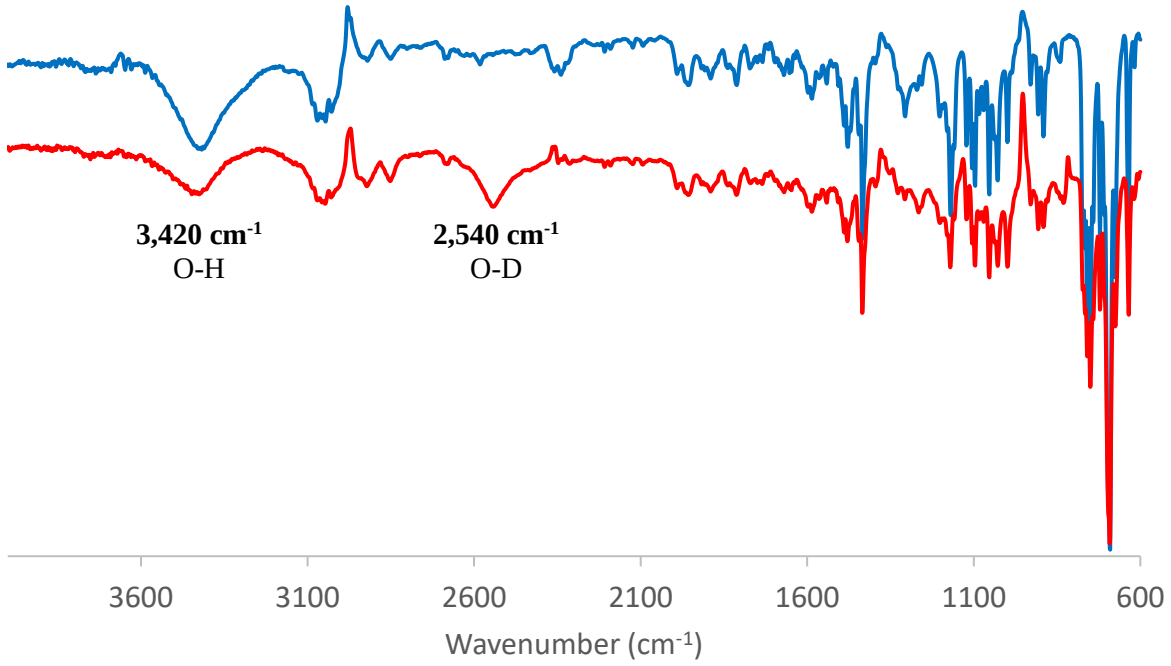

Figure S4. Blue trace: IR spectrum of **2** in the solid state. Red trace: IR spectrum of solid, deuterated **2** obtained by addition of MeOD to a DCM solution of **2** followed by *in vacuo* removal of solvent.

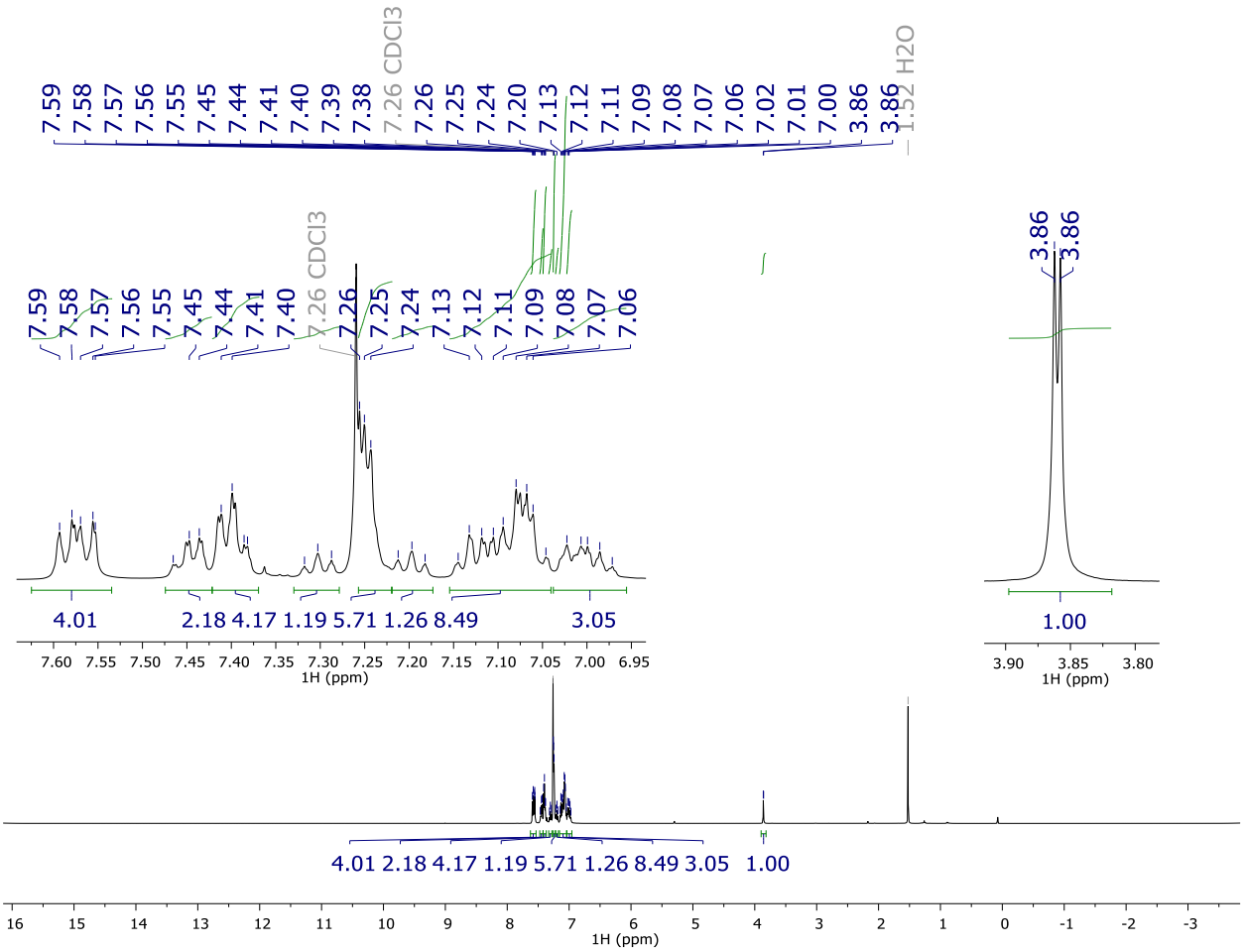

Figure S5. ^{1}H NMR spectrum of **3** in $CDCl_3$.

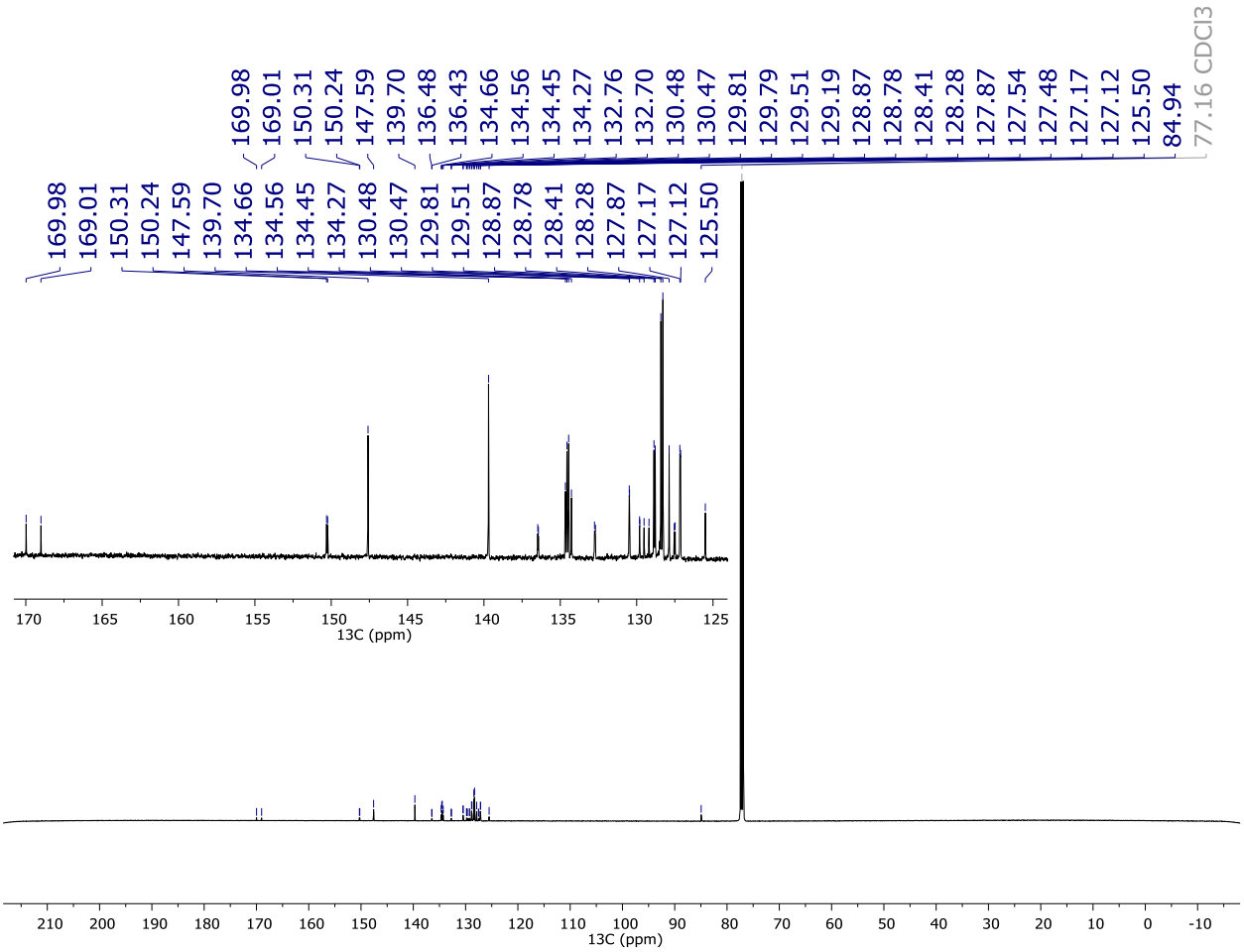

Figure S6. $^{13}C\{^{1}H\}$ NMR spectrum of **3** in $CDCl_3$.

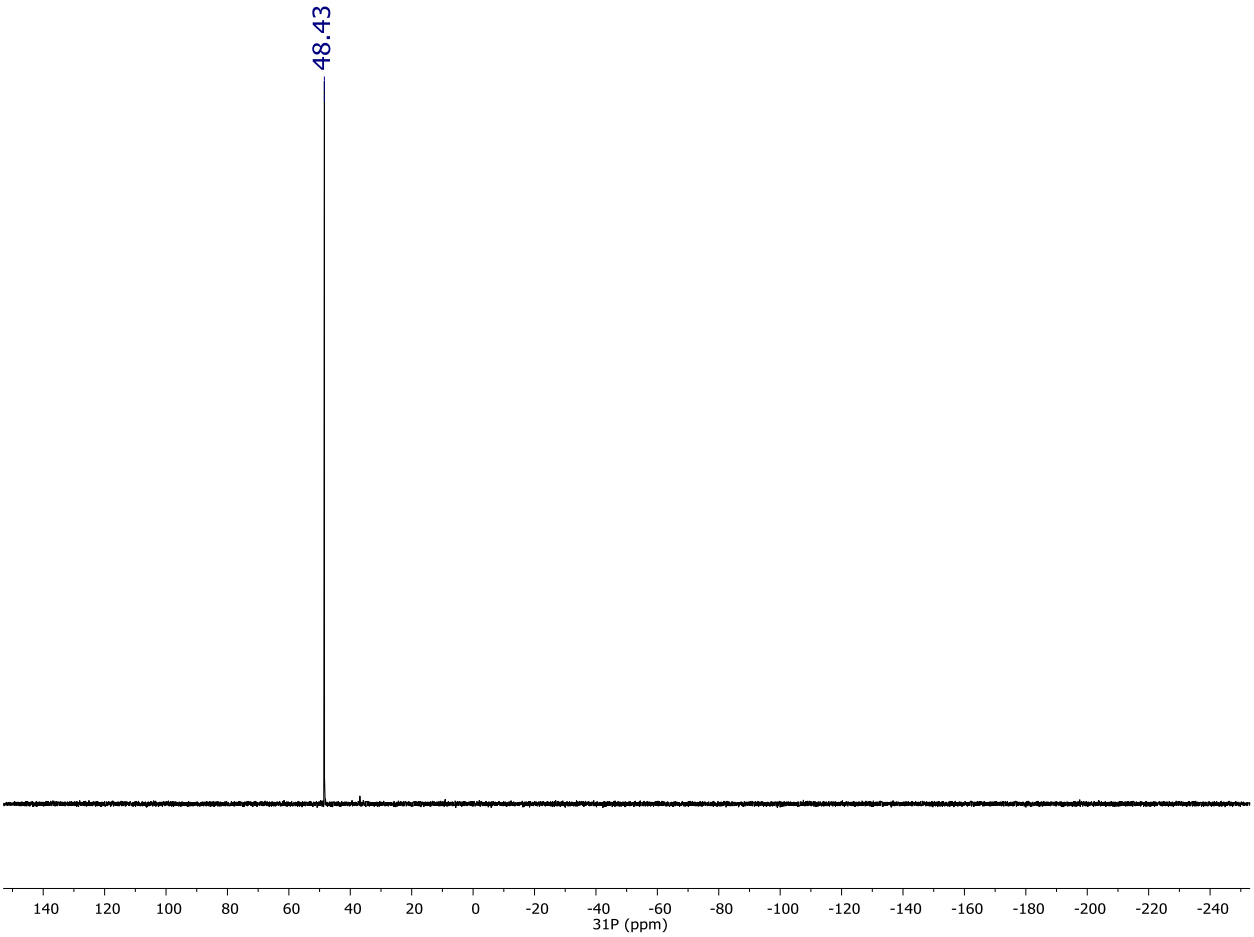

Figure S7. $^{31}P\{^{1}H\}$ NMR spectrum of **3** in $CDCl_3$.

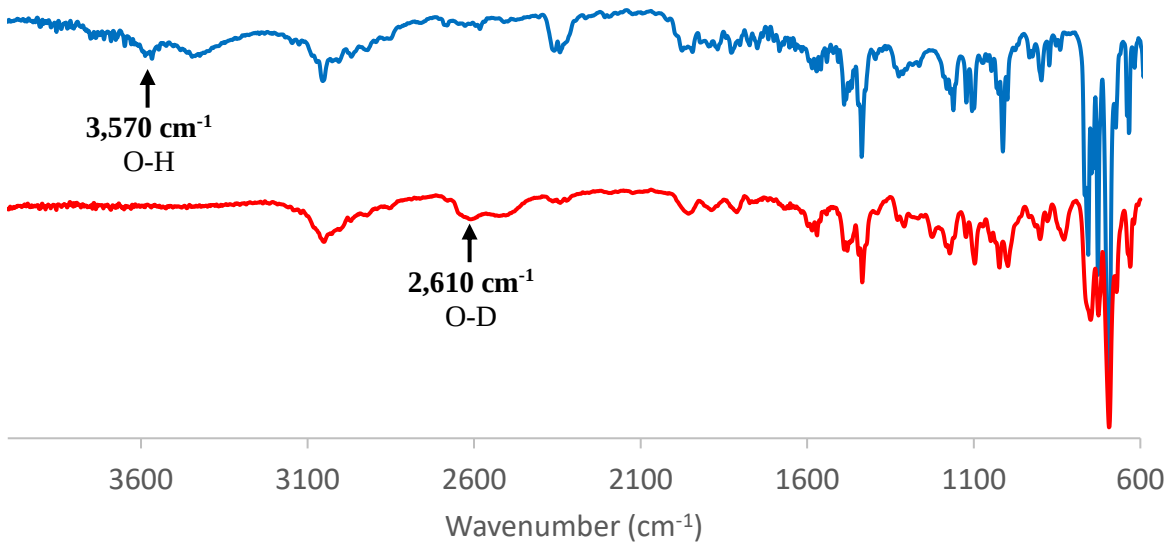

Figure S8. Blue trace: IR spectrum of **3** in the solid state. Red trace: IR spectrum of solid, deuterated **3** obtained by addition of MeOD to a DCM solution of **3** followed by *in vacuo* removal of solvent. O-H/D stretching peaks from residual **2** can be seen in both traces.

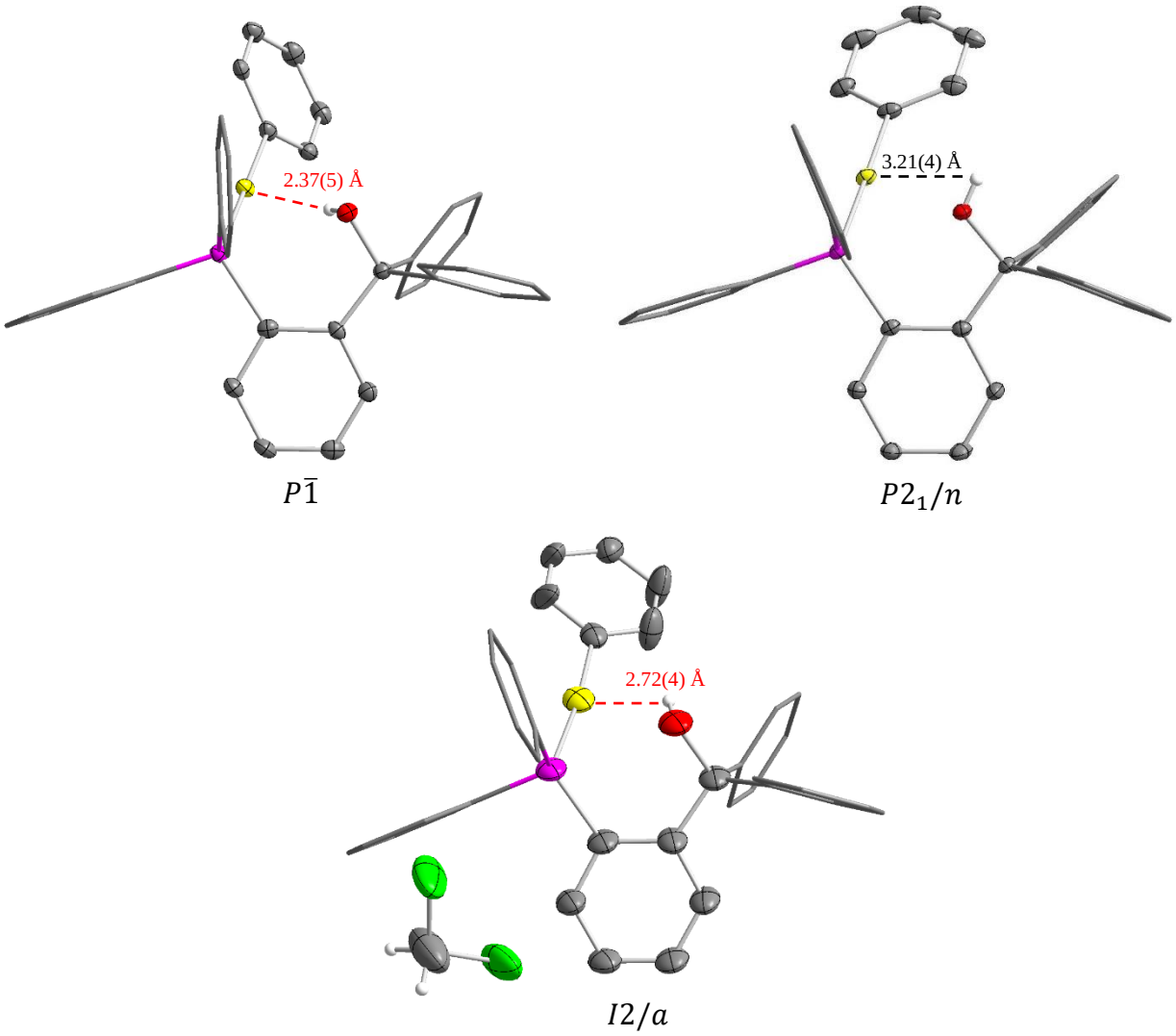

Figure S9. Crystal structures for polymorphs of **3**. Hydrogens other than O*H* and CH_2Cl_2 omitted for clarity. Thermal ellipsoids drawn at 50% probability, and phenyl groups drawn as thin lines (gray: C, red: O, magenta: P, green: Cl, white: H).

Computational Details

All calculations were carried out using density functional theory as implemented in the Gaussian 16 program.[9] All calculations were conducted with the mPW1PW91 functional and mixed basis sets (cc-pVTZ-PP[10] and ECP60 MDF[11] for Au; 6-31G(d',p') for P and Cl; and 6-31G(d,p) for all other atoms) starting from the crystal structure geometries. To switch off relativistic effects on gold, the non-relativistic basis set cc-pVTZ-PP-NR[10] with the ECP60 MHF[12] pseudopotential was used. No imaginary frequencies were found for the optimized structures, confirming that a local minimum on the potential energy hypersurface had been reached in all cases.

The computed OH/OD stretches were obtained by multiplying the computed harmonic frequencies by 0.94, a scaling factor, used as an approximate correction for force constant calculation errors and anharmonic effects. Such scaling factors are widely used.[13] In the present case, the value of 0.94 was derived from the experimental ν(OH) of methanol (3682 cm^{-1}) and that computed for the same compound (3904 cm^{-1}) at the above-mentioned level of theory.[13]

The computed ^{1}H NMR chemical shifts provided in the main text were obtained by application of the Gauge Including Atomic Orbitals (GIAO) method as implemented in the Gaussian program.[14-18] In all cases, the SMD solvation model was employed (with $CHCl_3$ selected as solvent). The computed isotropic ^{1}H chemical shifts are reported against those obtained for $SiMe_4$ at the same level of theory. These calculations were carried out at the above-mentioned level of theory.

Table S1. XYZ coordinates of the optimized geometry of **2a**.

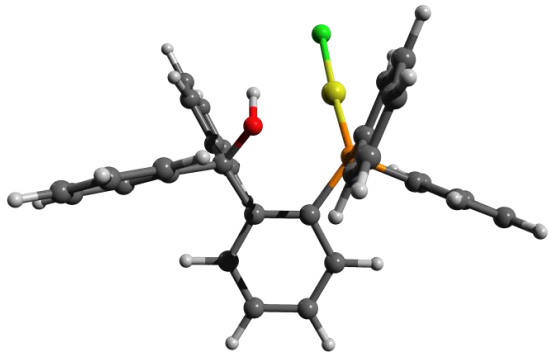

Au	-1.098670	1.592724	-0.608997	H	-4.983795	0.939544	2.881757
P	-1.206548	-0.565201	0.081530	C	-1.809589	-1.441743	-2.487488
Cl	-1.101149	3.743456	-1.383383	H	-2.186720	-0.433461	-2.630185
O	1.303939	-0.460175	-0.986539	C	-2.854225	-0.793650	0.871708
H	1.200427	0.393288	-1.425231	C	4.653644	-0.425241	0.472795
C	1.384493	-1.028613	1.310396	H	4.618193	0.451639	1.110704
C	-0.019740	-1.192758	1.357838	C	-0.737031	-3.094870	-1.091394
C	0.200951	-2.365206	3.488624	H	-0.278257	-3.378094	-0.150144
H	-0.269797	-2.882302	4.317541	C	1.933668	3.171994	1.875262
C	2.104877	-0.279842	0.180091	H	1.590651	3.609133	2.806847
C	2.804814	2.037200	-0.501847	C	1.816780	1.797321	1.678271
H	3.174476	1.596625	-1.423532	H	1.387763	1.180112	2.458803
C	2.242067	1.215532	0.484265	C	3.547257	-2.029648	-0.936808
C	-1.233254	-1.800434	-1.265742	H	2.639166	-2.399650	-1.398071
C	2.909619	3.408464	-0.309200	C	-5.359749	-1.030013	2.096588
H	3.333058	4.030359	-1.090029	H	-6.333414	-1.120011	2.566424
C	2.149414	-1.536690	2.363091	C	-1.890069	-2.369104	-3.521534
H	3.225767	-1.421185	2.325582	H	-2.335168	-2.080561	-4.467642
C	-0.580050	-1.866101	2.453546	C	-0.817975	-4.018602	-2.129532
H	-1.652914	-2.001962	2.502545	H	-0.426740	-5.020683	-1.988498
C	3.477258	-0.912309	-0.101087	C	5.875101	-1.046300	0.221546
C	1.576325	-2.193560	3.444853	H	6.779872	-0.651819	0.672193
H	2.207715	-2.572548	4.241282	C	-4.869454	-2.063742	1.304255
C	-3.360934	0.245751	1.661629	H	-5.459304	-2.961807	1.154281
H	-2.784046	1.157742	1.783831	C	-1.394280	-3.657845	-3.344595
C	-3.622633	-1.949321	0.695210	H	-1.452910	-4.378514	-4.153318
H	-3.251503	-2.758338	0.075767	C	4.767388	-2.646289	-1.190971
C	2.471554	3.981200	0.882187	H	4.806069	-3.509105	-1.847945
H	2.546990	5.052487	1.031555	C	5.936064	-2.158494	-0.611264
C	-4.602670	0.125111	2.275263	H	6.887868	-2.638645	-0.812590

Table S2. XYZ coordinates of the optimized geometry of **3a**. All polymorphs optimize to the same minimum-energy geometry.

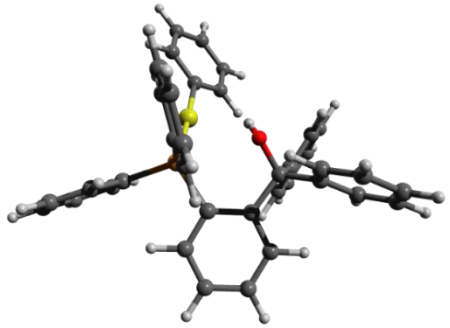

Au	1.739323	-0.268732	0.229060	H	-4.114815	0.948417	-3.867748
P	0.207580	1.475652	-0.120195	C	-0.497268	-3.599836	-2.448524
O	-1.338596	-0.533601	0.987740	H	-0.182909	-3.698951	-3.482099
C	3.133743	-1.718821	0.556204	C	-1.705078	2.903613	1.402557
C	4.255163	-1.481802	1.370501	H	-2.314328	2.926836	0.505112
H	4.380979	-0.512494	1.844961	C	-1.390624	3.478452	3.725844
C	0.301118	2.217604	2.557154	H	-1.750658	3.951507	4.633305
H	1.255413	1.699599	2.556010	C	5.095675	-3.713513	0.995192
C	-0.468650	2.251926	1.390866	H	5.847591	-4.478387	1.163397
C	2.127832	2.523627	-1.846859	C	-2.162646	3.513471	2.567601
H	2.300793	1.481891	-2.100824	H	-3.124969	4.014693	2.569322
C	3.031158	-2.992048	-0.030824	C	-1.296950	-3.322147	0.195095
H	2.181606	-3.223838	-0.665786	H	-1.614845	-3.214960	1.226938
C	-1.231347	1.230459	-1.260913	C	1.727792	5.189045	-1.160047
C	-1.067614	-2.402812	-2.016388	H	1.575241	6.226837	-0.882920
H	-1.190427	-1.586727	-2.718323	C	2.685571	4.854053	-2.112657
C	3.995550	-3.974935	0.183222	H	3.282032	5.630214	-2.580403
H	3.886541	-4.948967	-0.285630	C	-3.516371	-1.222258	0.400507
C	1.152835	2.851850	-0.895802	C	-2.411690	2.096929	-3.217698
C	-1.476860	-2.251581	-0.691895	H	-2.501103	2.853988	-3.989103
C	5.222158	-2.461055	1.589266	C	-0.726206	-4.512589	-0.234949
H	6.076461	-2.244572	2.224369	H	-0.592701	-5.328884	0.466686
C	0.963394	4.195184	-0.554615	C	-0.327222	-4.657212	-1.562778
H	0.222473	4.465922	0.189444	H	0.116940	-5.587381	-1.900811
C	-2.097628	-0.966321	-0.133771	C	-4.020363	-0.380466	1.395790
C	-2.149519	0.158510	-1.186210	H	-3.390044	0.406060	1.793908
C	-3.171258	0.095807	-2.140293	C	-4.327428	-2.247820	-0.087985
H	-3.887180	-0.715246	-2.079614	H	-3.944547	-2.923586	-0.845531
C	2.883759	3.519085	-2.456098	C	-5.620258	-2.424367	0.400987
H	3.635942	3.249810	-3.189763	H	-6.234899	-3.229496	0.011901
C	-0.158579	2.830333	3.718455	C	-6.115197	-1.581661	1.389731
H	0.443872	2.793963	4.619757	H	-7.119456	-1.722145	1.775496
C	-1.390973	2.182619	-2.280759	C	-5.308286	-0.560700	1.886825
H	-0.697033	3.011094	-2.345218	H	-5.682134	0.097172	2.664715
C	-3.307452	1.039424	-3.149000	H	-0.456985	-0.938738	0.947294

Table S3. XYZ coordinates of the optimized geometry of **3a**$_{\text{non-rel}}$.

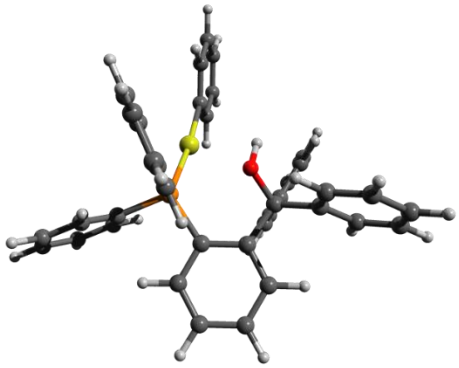

Au	1.737008	0.049320	0.146707	H	-4.960174	0.261710	-3.233746
P	-0.337744	1.523797	-0.056934	C	0.618485	-2.606716	-2.778893
O	-1.334082	-0.751196	1.025858	H	0.907055	-2.374142	-3.798575
C	3.600230	-1.084756	0.498974	C	-2.316029	2.343172	1.815812
C	4.115726	-1.298143	1.790429	H	-3.051353	2.148545	1.042782
H	3.596832	-0.887654	2.653864	C	-1.790672	3.059168	4.061074
C	-0.026230	2.360466	2.573197	H	-2.113576	3.422458	5.030959
H	1.028754	2.177234	2.388616	C	5.988552	-2.568951	0.947317
C	-0.961403	2.113981	1.562481	H	6.900012	-3.134066	1.118168
C	1.085111	3.008806	-1.934165	C	-2.726741	2.811985	3.060906
H	1.439741	2.034443	-2.259330	H	-3.781675	2.983208	3.248541
C	4.338550	-1.648604	-0.557579	C	-0.144227	-3.197203	-0.178992
H	3.995086	-1.523749	-1.581841	H	-0.456828	-3.460847	0.828051
C	-1.848017	1.046292	-1.022152	C	0.231289	5.509690	-1.072126
C	-0.411484	-1.885643	-2.175990	H	-0.096601	6.484557	-0.726622
H	-0.913803	-1.103136	-2.732536	C	1.112563	5.409558	-2.144906
C	5.509791	-2.376105	-0.345486	H	1.474348	6.306025	-2.637220
H	6.050851	-2.792094	-1.191752	C	-3.015865	-2.319562	0.340710
C	0.187913	3.096461	-0.862402	C	-3.516601	1.752844	-2.659281
C	-0.798850	-2.165437	-0.865575	H	-3.920934	2.531451	-3.297029
C	5.284524	-2.025617	2.017845	C	0.890099	-3.907024	-0.774989
H	5.646577	-2.166532	3.033064	H	1.396669	-4.688431	-0.219972
C	-0.230839	4.361370	-0.434577	C	1.276305	-3.611796	-2.080013
H	-0.915099	4.449056	0.402461	H	2.086563	-4.162175	-2.544921
C	-1.891392	-1.382421	-0.126641	C	-3.750801	-1.976052	1.478144
C	-2.446061	-0.235386	-0.981011	H	-3.486577	-1.076610	2.021832
C	-3.559782	-0.480936	-1.787085	C	-3.348298	-3.487932	-0.348956
H	-4.024303	-1.458798	-1.750805	H	-2.779322	-3.775025	-1.226922
C	1.538240	4.155908	-2.576510	C	-4.396790	-4.294535	0.087461
H	2.234400	4.070759	-3.404008	H	-4.639085	-5.200688	-0.457930
C	-0.438926	2.834220	3.814331	C	-5.122205	-3.946105	1.222033
H	0.296182	3.020563	4.589989	H	-5.934508	-4.577606	1.566057
C	-2.406583	2.017016	-1.865860	C	-4.794025	-2.784419	1.916447
H	-1.961154	3.003349	-1.906387	H	-5.350926	-2.507138	2.805534
C	-4.093986	0.492323	-2.622895	H	-0.601361	-1.287784	1.350471

Comparison of experimental and computational IR spectra

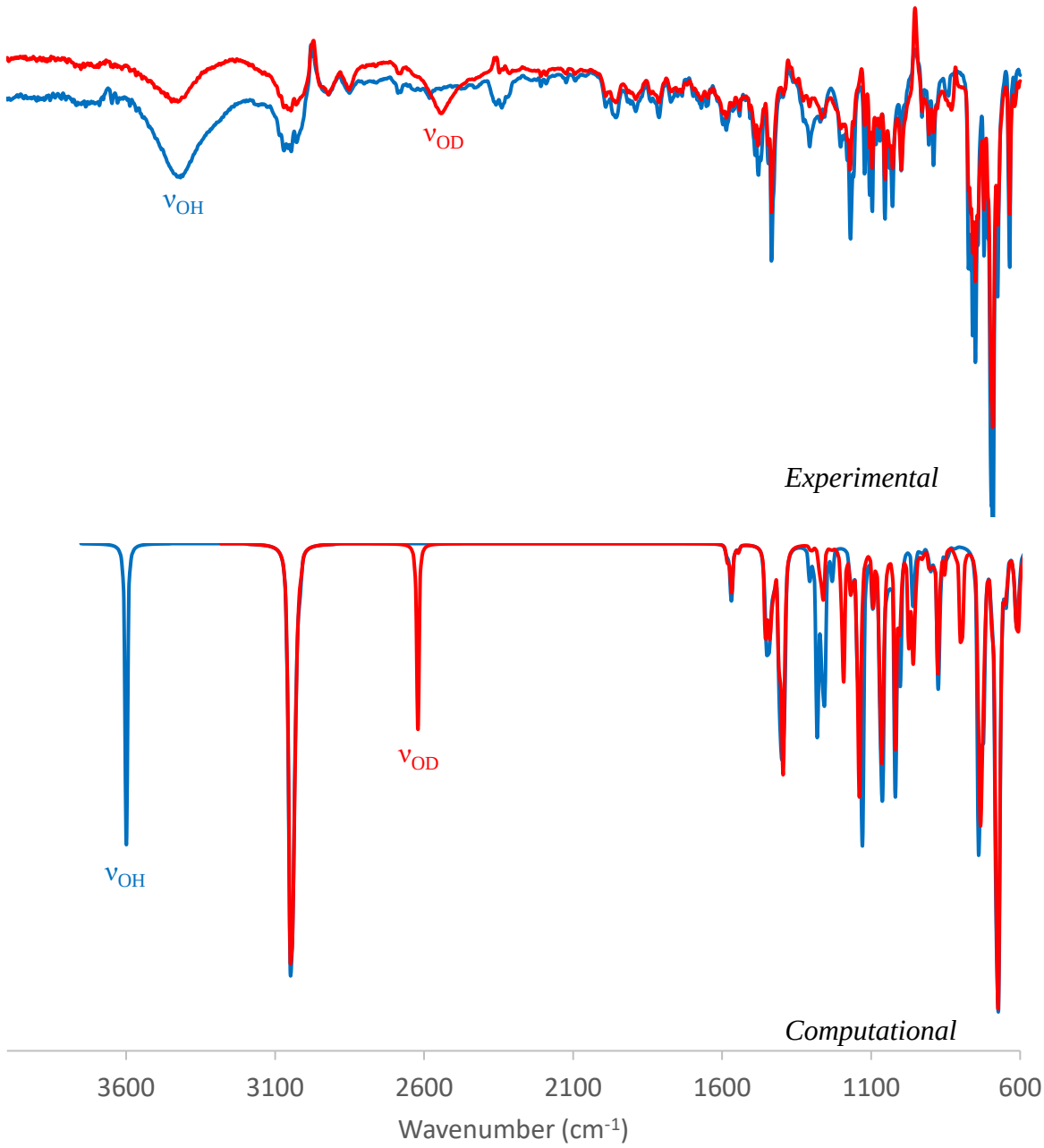

Figure S10. Top: Experimental IR spectra of **2** in the solid state before (blue) and after (red) deuteration. Bottom: Computational harmonic vibrational spectra of **2a** with (red) and without (blue) deuteration of the hydroxyl functionality. The computational spectra were corrected by multiplication of the harmonic frequencies by 0.94.

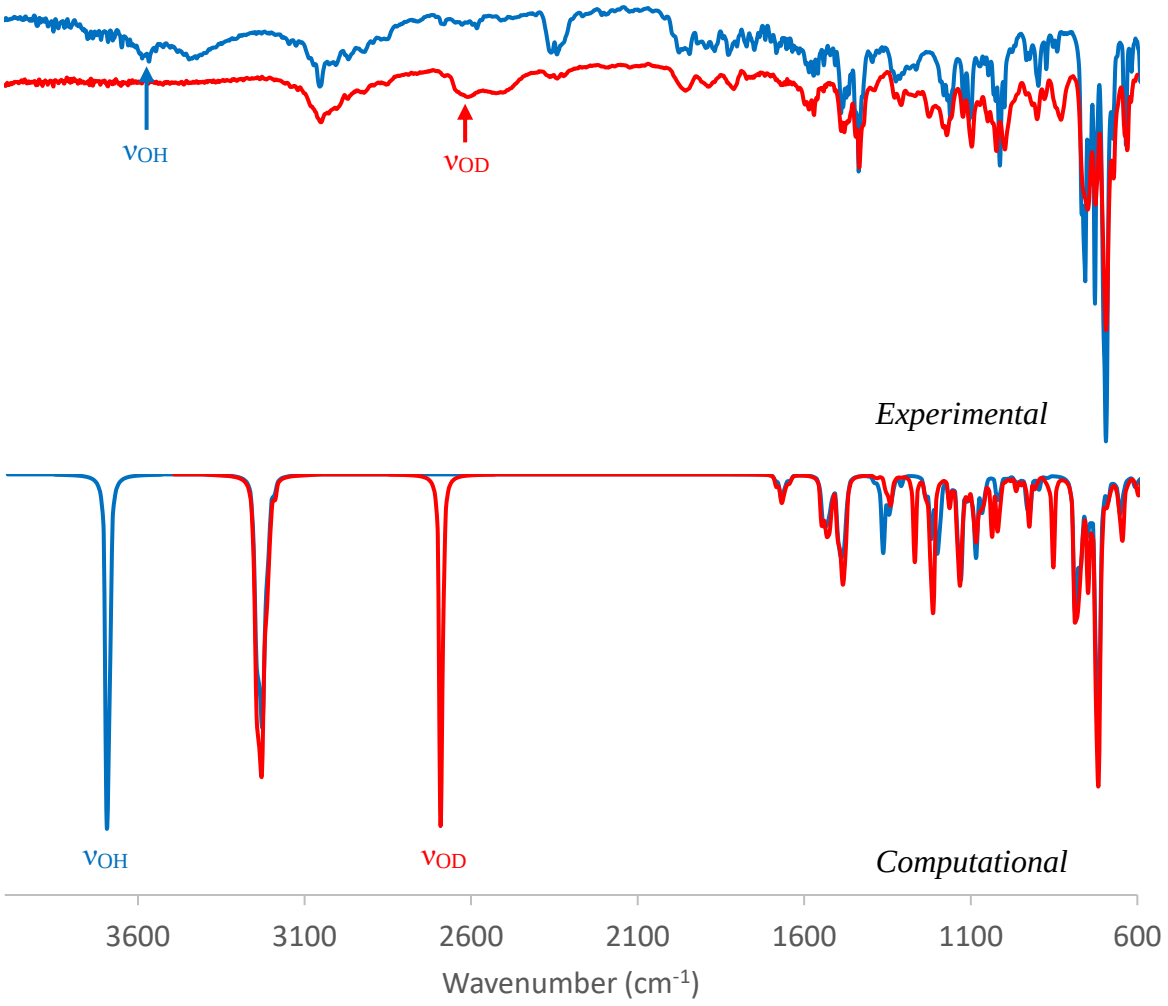

Figure S11. Top: Experimental IR spectra of **3** in the solid state before (blue) and after (red) deuteration. Bottom: Computational harmonic vibrational spectra of **3a** with (red) and without (blue) deuteration of the hydroxyl functionality. The computational spectra were corrected by multiplication of the harmonic frequencies by 0.94.

ESP Maps

Electrostatic Potential Surface (ESP) maps were created based on the optimized structures and plotted with GaussView 6.1.1.[19]

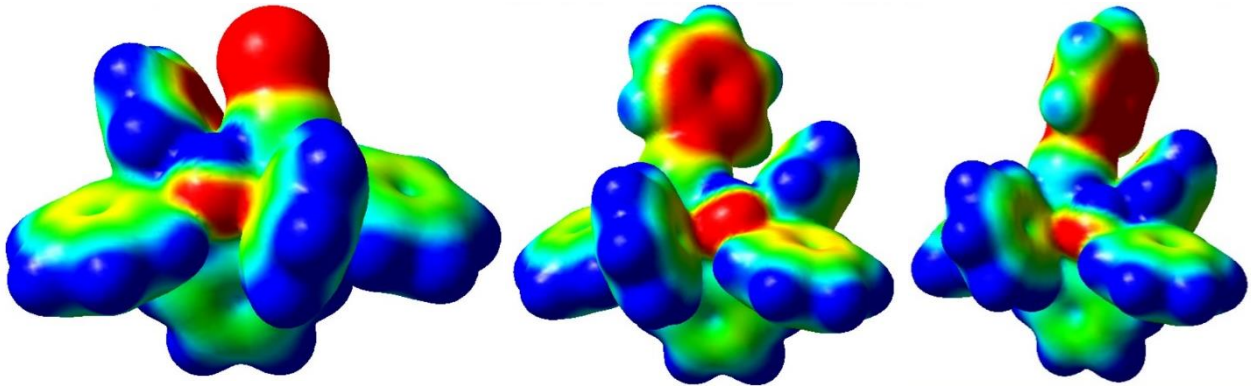

2a **3a** **3a$_{non-rel}$**

Figure S12. Electrostatic potential maps were plotted with a surface isovalue of 0.005 a.u. for **2a**, **3a**, and **3a$_{non-rel}$** (color scale: red, -0.04 a.u.; blue, 0.025 a.u.)

Natural Bond Orbital (NBO) Analysis

The optimized structures were also subjected to NBO analysis using NBO 7.[20] The NBOs were visualized and plotted using the Avogadro program.[21]

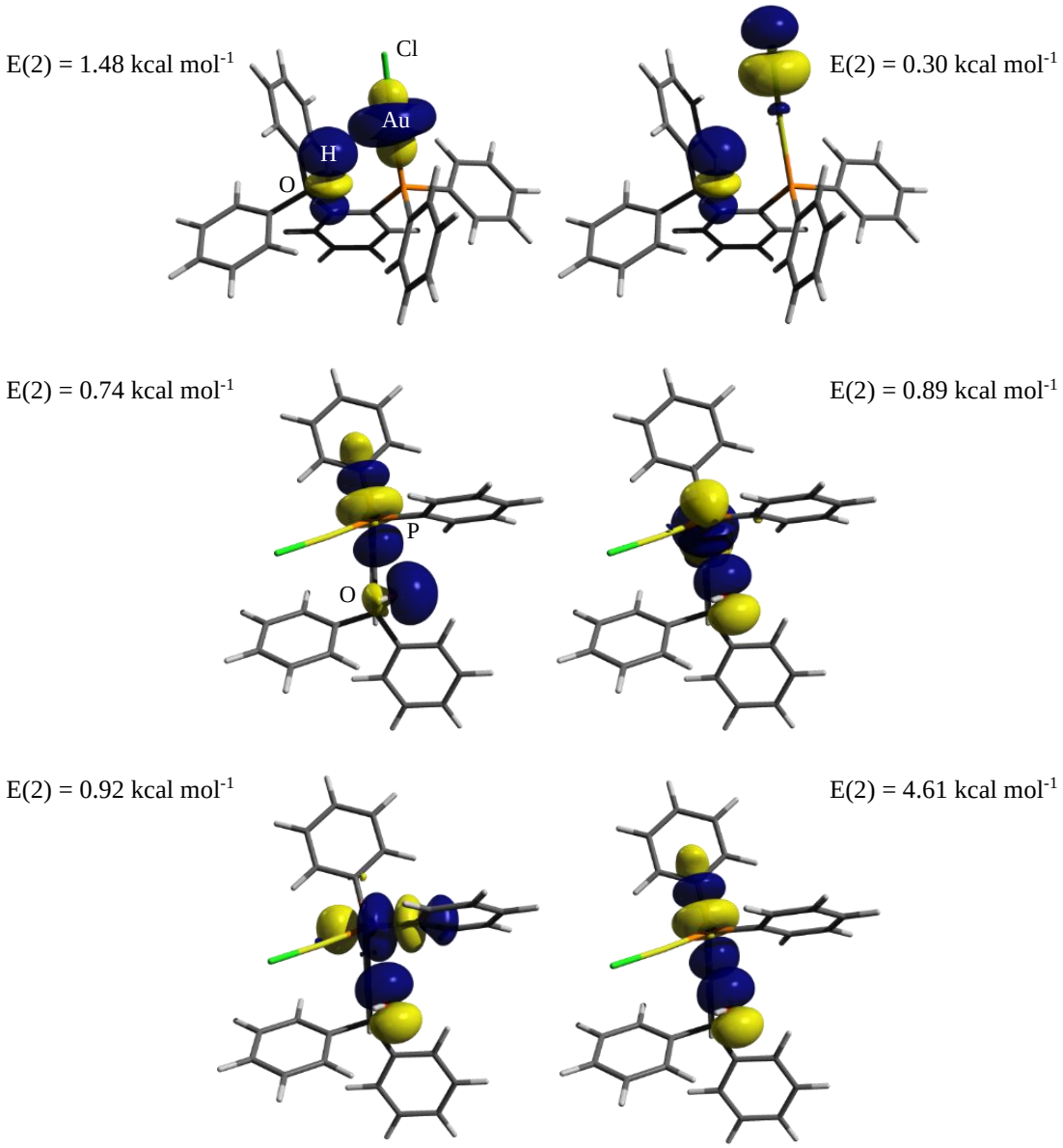

Figure S13. All lp(Au) → σ*(OH) and lp(O) → σ*(CP) donor-acceptor interactions (isovalue = 0.05) present in **2a**.

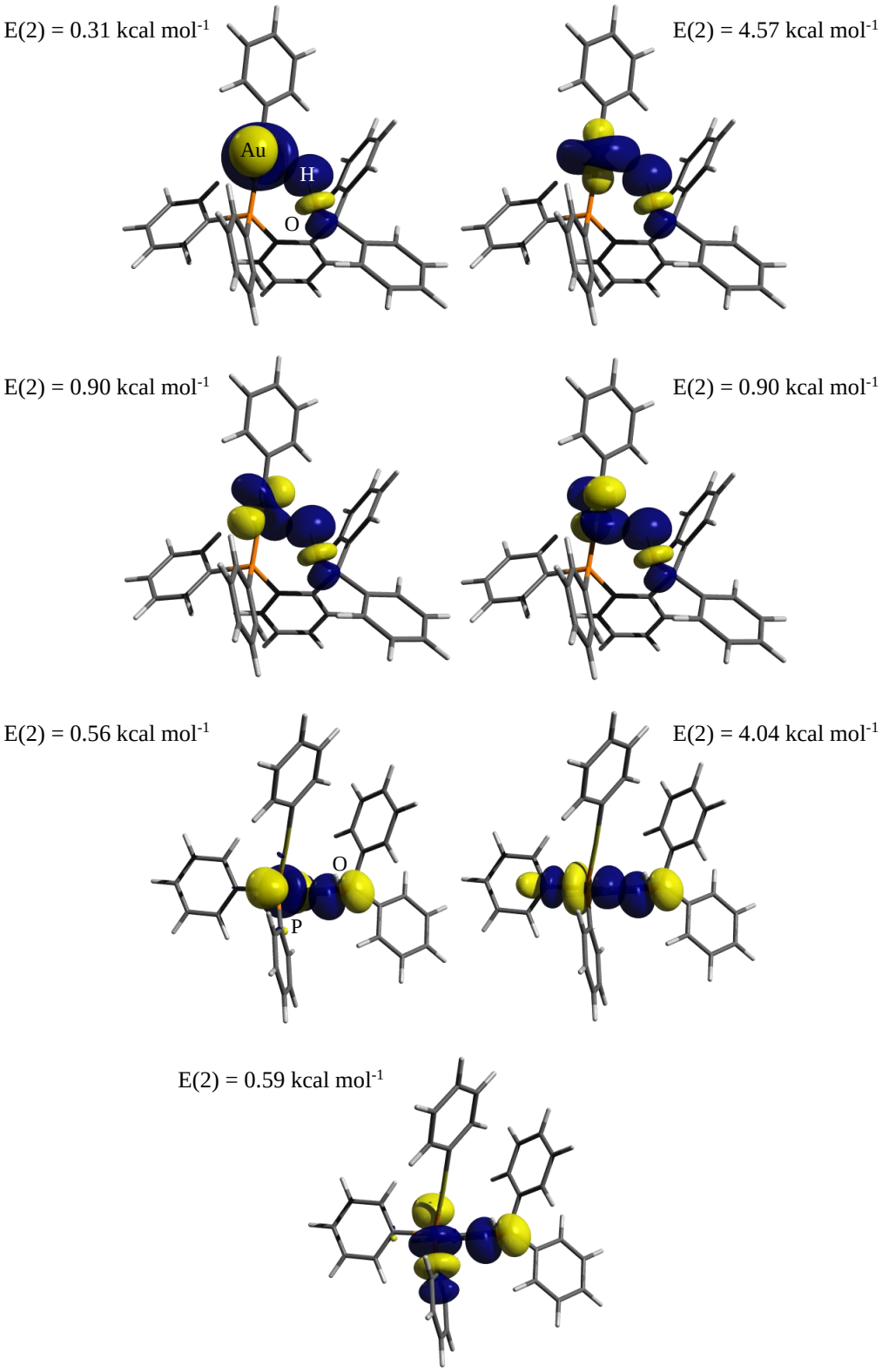

Figure S14. All lp(Au) → σ*(OH) and lp(O) → σ*(CP) donor-acceptor interactions (isovalue = 0.05) present in **3a**.

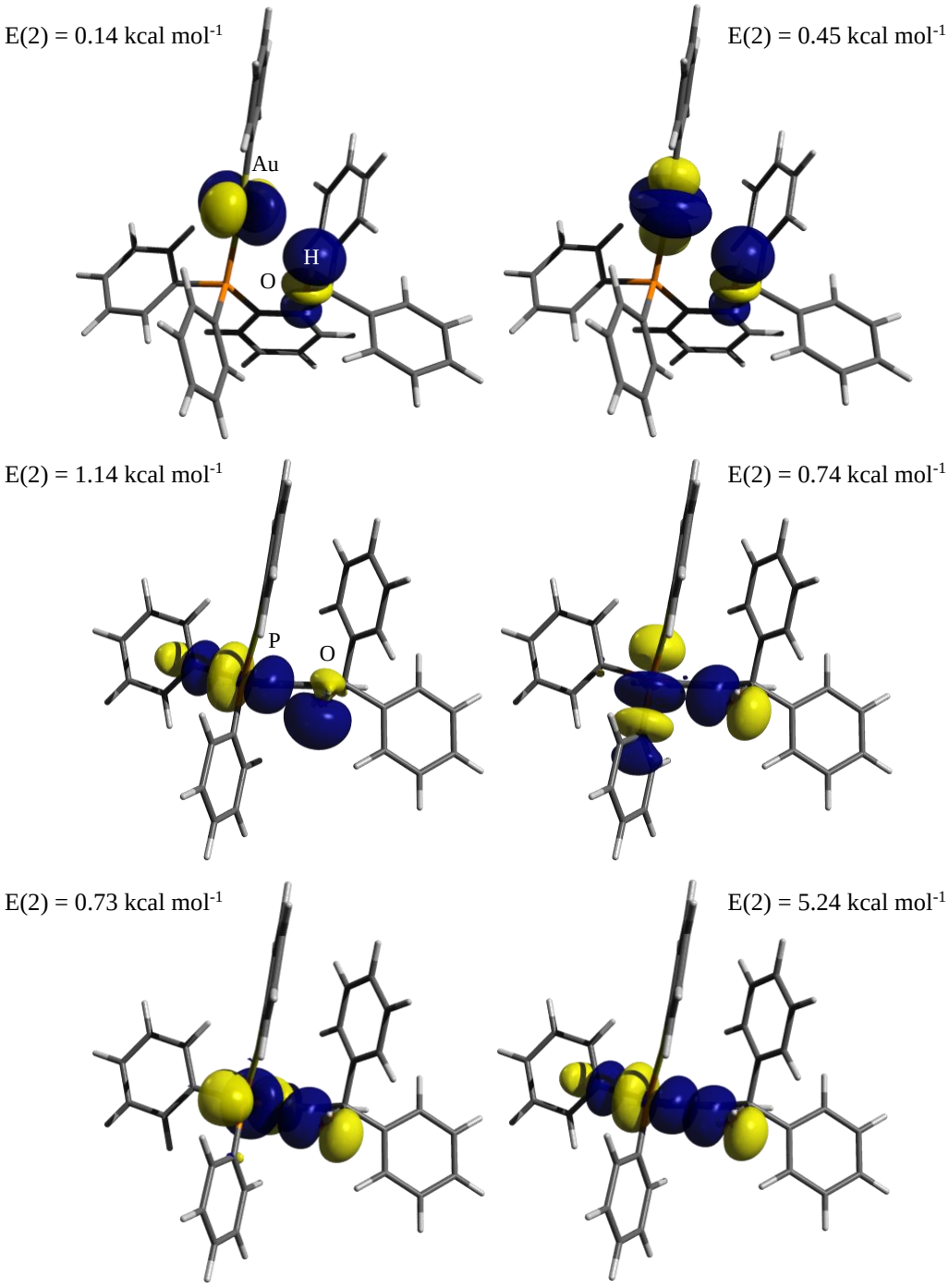

Figure S15. All lp(Au) → σ*(OH) and lp(O) → σ*(CP) donor-acceptor interactions (isovalue = 0.05) present in **3a**$_{\textbf{non-rel.}}$

Atoms-In-Molecules (AIM) Analysis

QTAIM calculations and NCIPLOT calculations were carried out on the wave functions derived from the optimized structures using the Mutiwfn program[22] and visualized using VMD.[23]

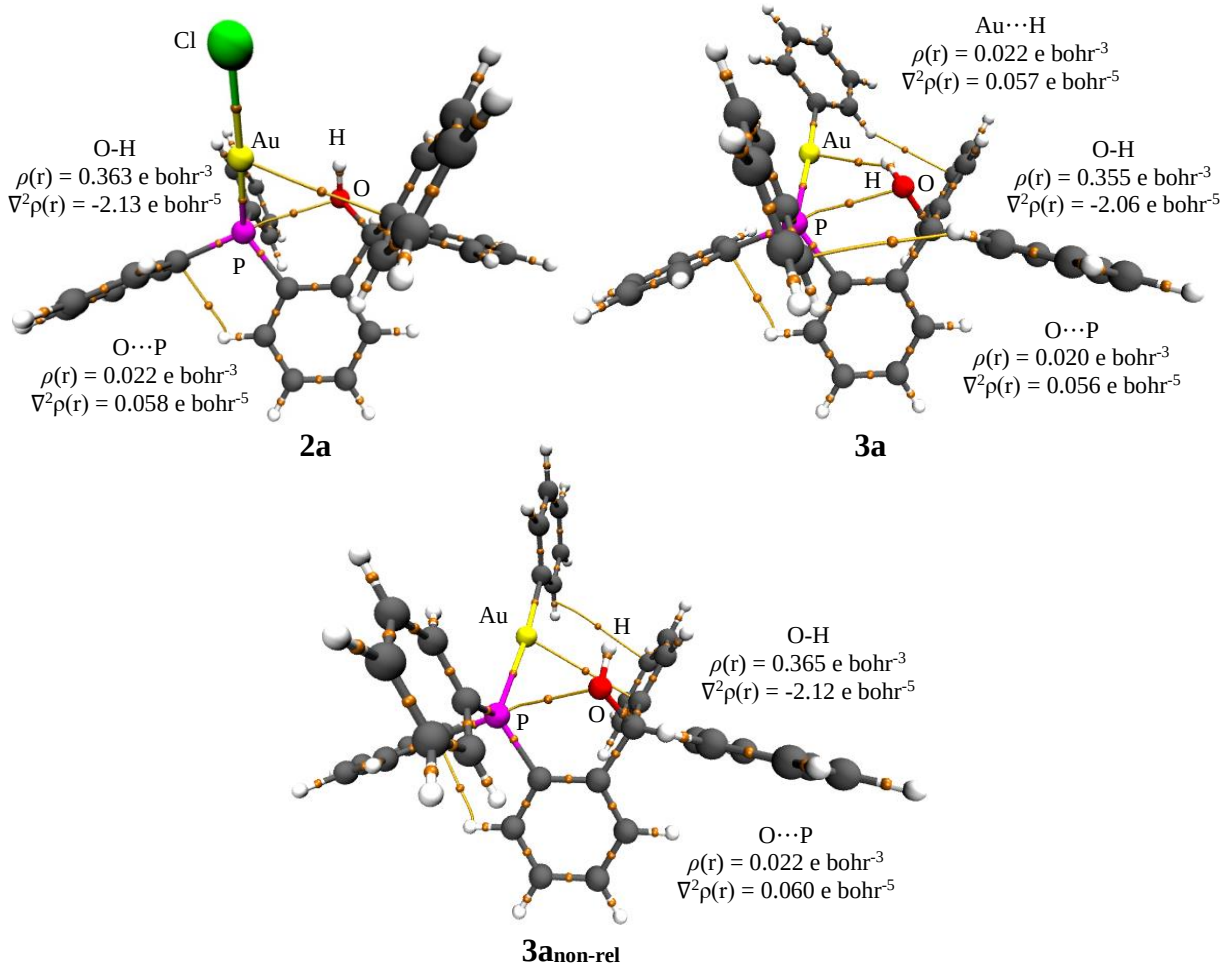

Figure S16. AIM output for compounds **2a** (top left), **3a** (top right), and **3a**$_{\textbf{non-rel}}$ (bottom), including all bond paths. (-3,+1) bond critical points omitted for clarity. Electron densities ($\rho(r)$ = e bohr^{-3}) and Laplacian distributions ($\nabla^2\rho(r)$ = e bohr^{-5}) provided for selected bond critical points.

NCI Plot with AIM Analysis

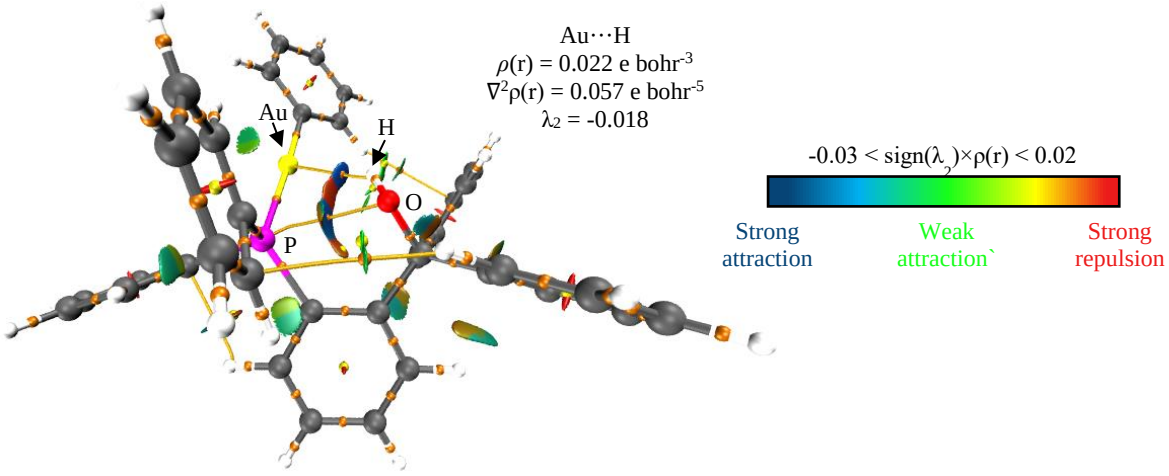

Figure S17. NCI plot with AIM analysis for **3a**. Gradient isosurface (0.3 a.u.) colored according to a blue-green-red scale with values in a.u.

References

1. K. Chansaenpak, M. Yang and F. P. Gabbaï, *Phil. Trans. R. Soc. A*, 2017, **375**, 20170007.
2. R. Uson, A. Laguna and M. Laguna, *Inorg. Synth.*, 1989, **26**, 85-91.
3. Bruker, 2019, APEX3 (v2019.2011-2010), Bruker AXS Inc., Madison, Wisconsin, USA
4. Rigaku Oxford Diffraction, (2022), *CrysAlisPro Software system*, version 171.42.61a, Rigaku Corporation, Wroclaw, Poland
5. G. M. Sheldrick, *SADABS, Version 2007/4, Bruker Analytical X-ray Systems, Inc., Madison, Wisconsin, USA*, 2007.
6. G. M. Sheldrick, *Acta Crystallogr., Sect. A*, 2015, **71**, 3-8.
7. G. M. Sheldrick *SHELXL-2014: Program for Crystal Structure Refinement*, University of Göttingen, Germany, 2014
8. O. V. Dolomanov, L. J. Bourhis, R. J. Gildea, J. A. K. Howard and H. Puschmann, *J. Appl. Crystallogr.*, 2009, **42**, 339-341.
9. M. J. Frisch, G. W. Trucks, H. B. Schlegel, G. E. Scuseria, M. A. Robb, J. R. Cheeseman, G. Scalmani, V. Barone, G. A. Petersson, H. Nakatsuji, X. Li, M. Caricato, A. V. Marenich, J. Bloino, B. G. Janesko, R. Gomperts, B. Mennucci, H. P. Hratchian, J. V. Ortiz, A. F. Izmaylov, J. L. Sonnenberg, Williams, F. Ding, F. Lipparini, F. Egidi, J. Goings, B. Peng, A. Petrone, T. Henderson, D. Ranasinghe, V. G. Zakrzewski, J. Gao, N. Rega, G. Zheng, W. Liang, M. Hada, M. Ehara, K. Toyota, R. Fukuda, J. Hasegawa, M. Ishida, T. Nakajima, Y. Honda, O. Kitao, H. Nakai, T. Vreven, K. Throssell, J. A. Montgomery Jr., J. E. Peralta, F. Ogliaro, M. J. Bearpark, J. J. Heyd, E. N. Brothers, K. N. Kudin, V. N. Staroverov, T. A. Keith, R. Kobayashi, J. Normand, K. Raghavachari, A. P. Rendell, J. C. Burant, S. S. Iyengar, J. Tomasi, M. Cossi, J. M. Millam, M. Klene, C. Adamo, R. Cammi, J. W. Ochterski, R. L. Martin, K. Morokuma, O. Farkas, J. B. Foresman and D. J. Fox *Gaussian 16 Rev. C.01*, Wallingford, CT, 2016
10. K. A. Peterson and C. Puzzarini, *Theor. Chem. Acc.*, 2005, **114**, 283-296.
11. D. Figgen, G. Rauhut, M. Dolg and H. Stoll, *Chem. Phys.*, 2005, **311**, 227-244.
12. P. Schwerdtfeger, M. Dolg, W. H. E. Schwarz, G. A. Bowmaker and P. D. W. Boyd, *Chem. Phys.*, 1989, **91**, 1762-1774.
13. G. Park and F. P. Gabbaï, *J. Am. Chem. Soc.*, 2021, **143**, 12494-12498.
14. F. London, *J. Phys. Radium*, 1937, **8**, 397-409.
15. R. McWeeny, *Phys. Rev.*, 1962, **126**, 1028-1034.
16. R. Ditchfield, *Mol. Phys.*, 1974, **27**, 789-807.
17. K. Wolinski, J. F. Hinton and P. Pulay, *J. Am. Chem. Soc.*, 1990, **112**, 8251-8260.
18. J. R. Cheeseman, G. W. Trucks, T. A. Keith and M. J. Frisch, *Chem. Phys.*, 1996, **104**, 5497-5509.
19. R. Dennington, T. Keith and J. Millam *GaussView*, Semichem Inc., Shawnee Mission, KS, 2019
20. E. D. Glendening, J. K. Badenhoop, A. E. Reed, J. E. Carpenter, J. A. Bohmann, C. M. Morales, P. Karafiloglou, C. R. Landis and F. Weinhold *NBO 7.0*, Theoretical Chemistry Institute, University of Wisconsin, Madison, 2018
21. M. D. Hanwell, D. E. Curtis, D. C. Lonie, T. Vandermeersch, E. Zurek and G. R. Hutchison, *J. Cheminf.*, 2012, **4**, 17.
22. T. Lu and F. Chen, *J. Comput. Chem.*, 2012, **33**, 580-592.
23. W. Humphrey, A. Dalke and K. Schulten, *J. Mol. Graphics*, 1996, **14**, 33-38.